Role of Protein−Protein Bridging Interactions on Cooperative Assembly of DNA-Bound CRP−CytR−CRP Complex and Regulation of the *Escherichia Coli* CytR Regulon†

Mayy Chahla,‡ John Wooll,§ Thomas M. Laue,§ Nghia Nguyen,‡ and Donald F. Senear*,‡

Department of Molecular Biology and Biochemistry, University of California, Irvine, California 92697, and Department of Biochemistry, University of New Hampshire, Durham, New Hampshire 03824

Received November 5, 2002; Revised Manuscript Received February 10, 2003

ABSTRACT: The unlinked operons that comprise the *Escherichia coli* CytR regulon are controlled coordinately through interactions between two gene regulatory proteins, the cAMP receptor protein (CRP) and the cytidine repressor (CytR). CytR controls the balance between CRP-mediated recruitment and activation of RNA polymerase and transcriptional repression. Cooperative interactions between CytR, when bound to an operator (CytO) located upstream of a CytR-regulated promoter, and CRP, when bound to flanking tandem promoters, are critical to the regulatory role of CytR. When CytR binds cytidine, cooperativity is reduced resulting in increased transcriptional activity. However, this cytidine-mediated effect varies among promoters, suggesting that coupling between cytidine binding to CytR and CytR−CRP association is sensitive to promoter structure. To investigate the chemical and structural basis for these effects, we investigated how cytidine binding affects association between CytR and CRP in solution and how it affects the binding of CytR deletion mutants lacking the DNA binding HTH domain, with tandem CRP dimers bound to either *udpP* or *deoP2*. Deletion mutants that, as we show here, retain the native functions of the allosteric, inducer-binding domain but do not bind DNA were expressed and purified. We refer to these as Core domain. Despite only weak association between CytR and CRP in solution, our results demonstrate the formation of a relatively stable complex in which the Core domain forms a protein bridge between tandem CRP dimers when bound to either *udpP* or *deoP2*. The ΔG° for bridge complex formation is about −7.8 kcal/mol. This is well in excess of that required to account for cooperativity (−2.5 to −3 kcal/mol). The bridge complexes are significantly destabilized by cytidine binding, and to the same extent in both promoter complexes ($\Delta\Delta G^\circ \approx +2$ kcal/mol). Even with this destabilization, ΔG° for bridge complex formation by cytidine-liganded Core domain is still sufficient by itself to account for cooperativity. These findings demonstrate that direct coupling between cytidine binding to CytR and CytR−CRP association does not account for promoter-specific effects on cooperativity. Instead, cytidine binding must induce a CytR conformation that is more rigid or in some other way less tolerant of the variation in the geometric arrangement of operator sites between different promoters.

Combinatorial control of multiple, unlinked genes is a ubiquitous feature of gene regulation. Typically, both relatively common transcription factors and also factors that are specific to a particular gene, tissue, or cell type to developmental stage or a particular metabolic state are involved. By combining specific factors with more ubiquitous factors, entire programs of gene expression can be triggered by a cascade effect when the functional state of one or a few specific factors is changed as a result of ligand binding, covalent modification, protein processing, or nuclear transport. Differential control of individual genes is provided within the context of coordinate control by variable arrays of DNA binding sites as are found in different promoters. These can direct different interactions, even among the same transcription factors, resulting in different effects on the basal transcription machinery.

The CytR[1] regulon of *Escherichia coli* is a relatively simple bacterial system that utilizes these basic aspects of combinatorial regulation to coordinate the expression of nine unlinked transcription units that encode the proteins and enzymes required for transport and utilization of nucleosides (*1*, *2*). Transcription of these genes is activated in response to intracellular cAMP levels by the cAMP receptor protein (CRP), a transcription factor that activates expression of over 100 *E. coli* genes. Transcription is repressed by the cytidine repressor protein (CytR), a regulon-specific member of the

† This work was supported by National Science Foundation by Grants MCB-9728186 to D.F.S. and DBI 9876582 to T.M.L.

* To whom correspondence should be addressed. Tel.: (949) 824-8014. E-mail: dfsenear@uci.edu.

‡ University of California.

§ University of New Hampshire.

[1] Abbreviations: αCTD, α-subunit of *E. coli* RNA polymerase; bp, base pair; cAMP, cyclic-5′,3′-adenosine monophosphate; CRP, *E. coli* cAMP receptor protein; CRP1 and CRP2, proximal and distal CRP operators, respectively; CytO, CytR operator site; CytR, *E. coli* cytidine repressor protein; Core domain, CytR mutants with N-terminal, DNA binding domain deleted; *deoP2*, *E. coli* proximal *deo* promoter; dNTP, 5′-deoxyribonucleotide triphosphate; *udpP*, *E. coli* uridine dephosphorylase promoter.

10.1021/bi0271143 CCC: $25.00
Published on Web 03/11/2003

LacR family of homologous bacterial repressors (*3*). Expression is induced when CytR binds an effector ligand, cytidine.

An important feature of the regulation mediated by CytR and CRP is that extents of activation, repression, and induction vary among the promoters, even among those with a similar arrangement of regulatory elements and similar binding affinities for the two proteins (*4*−*6*). To understand the combinatorial control mediated by CytR and CRP at the molecular level, we need to know how these transcription factors interact with each other and with RNA polymerase (RNAP) to control the assembly and activity of functional transcription complexes at the different CytR-regulated promoters. As this prokaryotic example illustrates, the molecular mechanisms of combinatorial control are fundamental to genetic expression in all organisms.

Most CytR-regulated promoters contain tandem CRP operators, CRP1 and CRP2. CRP bound to these sites is thought to activate transcription via two distinct interactions with RNAP (reviewed in ref *7*). First, both CRP1-bound CRP and CRP2-bound CRP contact the C-terminal domain of the α-subunit of the polymerase (αCTD) to facilitate its binding to the intervening DNA. Second, allosteric interactions between the CRP1-bound CRP and the α N-terminal domain accelerates initiation. The operator for CytR (CytO) is located between CRP1 and CRP2. It has long been assumed that CytR binding in this location occludes the interactions between CRP and αCTD.

A key to CytR-mediated regulation is that despite roles as functional antagonists, CytR and CRP bind with positive cooperativity to their respective operators (*8*, *9*). Cooperativity is pairwise when only one CRP is bound. But a three way cooperative complex also forms in which CytR forms a protein bridge between tandem, DNA-bound CRP dimers. In this complex, CytR is expected to compete with αCTD both for DNA binding and association with CRP. Consistent with the expectation that cooperativity should enhance the activity of CytR as an αCTD antagonist, the three protein, CRP−CytR−CRP complex is required for repression; CytR alone does not repress basal level transcription (*1*). Further underscoring the critical role of cooperativity in stabilizing the three-protein repression complex is the mechanism of induction. Cytidine binding to CytR results in a decrease in cooperativity but has little or no effect on the intrinsic affinity of CytR for binding to CytO (*9*, *10*). Thus, cooperativity provides the underlying basis for both repression and induction.

However, the response to cytidine differs at different promoters. At *deoP2*, cooperativity is eliminated (*9*, *10*), thus reducing the overall affinity for CytR binding by over 100-fold. In contrast, the interaction between CytR and CRP bound to CRP2 of *udpP* is virtually unaffected by cytidine (*11*) resulting in only a small decrease in overall CytR binding affinity. Consequently, CytR remains associated to similar extents under inducing and repressing conditions. Yet, induction of *udpP* is unusually effective, resulting in a 60-fold increase in expression (*4*). Evidently, dissociation of CytR is not necessary for induction of *udpP* nor is association sufficient for repression.

The significance of this behavior might be explained by the results of a recent study of CytR-mediated repression of *deoP2* (*6*). The three-protein CRP−CytR−CRP complex was shown not only to reverse CRP-mediated activation but also to actively block basal level activity, reducing transcription to a level significantly below that in the absence of CRP. This suggests that interaction with CytR converts CRP from an activator to a repressor. Thus, it appears that CytR not only occludes interactions involving RNAP αCTD as a result of bridging interactions but also modulates the activity of CRP1-bound CRP. In view of this result, the significance of the difference in response to cytidine at different promoters is easy to understand.

The underlying question is what accounts for the difference in response to cytidine. This difference was an unexpected finding, following our previous investigation of the allosteric linkage between cytidine binding to CytR and cooperativity (*4*). The results of those studies indicated that cytidine is an allosteric effector of only two functional states. Loss of cooperativity correlates with binding of only a single cytidine to either, but not both, subunits of CytR dimer. On the basis of the view that the thermodynamic driving force for cooperativity is CytR−CRP association, the presumption was that cytidine binding induces a concerted change in the conformation of the CytR dimer, the result of which is to decrease greatly its affinity for association with CRP. But the fact that CytR−CRP2 cooperativity is retained at *udpP* and perhaps also at other promoters (*12*) contradicts this simple interpretation.

Since CytR and CRP bind in a cooperative manner, the separate interactions between CytR and CytO, and between CytR and both CRP1-bound and CRP2-bound CRP, must combine to yield a net free energy change that is more favorable than for any of these individual interactions. For example, this would be the case if the free energy change for formation of the three-protein repression complex equaled the sum of free energy changes for each of the component pairwise interactions. But observations made several years ago using truncation mutants of CytR that lack the N-terminal DNA-binding domain suggest that CytR−CRP and CytR−CytO interactions may not combine quite so favorably as this. Overexpression of these mutants in a *cytr* strain was shown to repress CytR regulated genes (*13*). This was interpreted to indicate that CytR mutants associate via bridging protein−protein interactions alone to form a functional, DNA-bound CRP−CytR−CRP repression complex. This interpretation implies an affinity for CytR bridging that is much higher than what might be expected based on the cooperativity when full-length CytR binds CytO. The net cooperative free energy change is approximately −2.5 to −3 kcal/mol (*9*, *11*). This would correspond to a k_d of only 10 mM, or far too low to compete effectively with αCTD binding to cause repression. This comparison suggests a high affinity for CytR bridging alone, which must be counterbalanced by another, thermodynamically unfavorable process when CytR both bridges and binds CytO. The result appears to be a surprisingly small net difference between the combined ΔG for these interactions and the ΔG for either alone.

The specific geometric arrangement of CytR and CRP binding sites in any promoter constitutes a scaffold for individual protein−DNA and protein−protein interactions. Such a scaffold should influence how the energetic contributions of individual interactions are combined. The individual interactions will combine favorably when the conformation of the DNA-binding and allosteric domains of CytR matches

the arrangement or operators at a particular promoter. Even in the absence of cytidine, the CytR conformation must not be optimal, as the relatively weak cooperativity attests. But this state of CytR must be relatively tolerant of the differences between *deoP2* and *udpP* because the cooperative ΔG is similar (*9*, *11*). Our hypothesis is that the cytidine liganded state is less tolerant of the differences between the promoters, accounting for much different effects on CytR−CRP cooperativity.

To test this hypothesis, we have investigated how cytidine affects the interplay between CytR−DNA and CytR−CRP interactions. This was done by comparing the energetics of CytR−CRP association to the energetics of cooperativity when CytR and CRP bind to *deoP2* and to *udpP* both in the presence and in the absence of cytidine. If cytidine is an allosteric effector of CytR−CRP association, there will be an effect on the solution assembly reaction. On the other hand, if cytidine does not affect the solution assembly but instead affects either bridge formation or cooperativity, this would indicate an effect on geometric constraints as a consequence of the scaffolding. To assess the contributions from these different processes, we have determined the free energy change for solution assembly of free and DNA-bound CytR and CRP dimers using sedimentation equilibrium analysis and the energetics of protein bridging using DNase I footprinting. To evaluate the energetics of the protein bridging reactions in the absence of CytR−DNA interaction, we expressed and purified CytR deletion mutants that lack the entire DNA-binding HTH domain but that, as we show here, retain the functions of the allosteric, inducer-binding domain. Following the nomenclature used in the PurR and LacR literature (*14*, *15*), we denote these CytR deletion mutants as Core domain. DNase I footprint analysis was used to investigate the binding of CytR Core domain proteins to CRP_2−*deoP2* and to CRP_2−*udpP* complexes. We compare the energetics for these associations to what we have determined previously for cooperative binding of full-length wild-type CytR to CRP_2−*deoP2* and to CRP_2−*udpP* complexes (*9*, *11*).

The results indicate only weak association between free CytR and CRP to form a hetero-tetrameric complex in solution. By contrast, functional CytR Core domain dimers that do not bind DNA form relatively stable bridged complexes with both CRP_2−*deoP2* and CRP_2−*udpP*. The bridged complexes are destabilized by cytidine but to the same extent at the two promoters. While this effect is in the correct direction to account for decreased cooperativity when cytidine binds, it cannot account for the promoter-specific effects. These results support our hypothesis that cytidine is an allosteric effector of CytR conformations that constrain its simultaneous association with CytO and the flanking CRP dimers.

MATERIALS AND METHODS

Reagents and Enzymes. Crystalline cAMP (free base, >99% pure) was purchased from Boehringer Manheim. Crystalline cytidine (>99% pure as free acid) was purchased from Sigma. Stocks were prepared in 50 mM bisTris, pH 7.0, 1 mM EDTA and stored at −80 °C. Stock concentrations were determined, and purity was assessed spectrophotometrically as described previously (*9*). Easytide [α-^{32}P]-dNTPs (3000 Ci/mmol) were purchased from NEN DuPont; unlabeled dNTPs were from Gibco/BRL. [5-^{3}H]-cytidine (ca. 18 Ci/mmol; >99.8% radiochemical purity) was purchased from Moravek Biochemicals. Buffer components and reagents were electrophoresis grade if available and reagent grade otherwise.

CRP and CytR Purification. The CRP and wild-type CytR preparations used in these experiments have been described previously (*4*, *9*). CRP, overexpressed from plasmid pPLcCRP1 (*16*) in *E. coli* strain K12 ΔHΔtrp, was isolated to at least 98% purity and stored at −80 °C in 50 mM bisTris, pH_4 7.85, 0.1 M KCl, 1 mM Na_4EDTA, 1 mM DTT, 1 mM NaN_3, 10% (v/v) glycerol. CytR was expressed and purified to at least 95% purity as described (*4*). Purified CytR in a buffer containing 20 mM MOPS, pH_4 6.80, 2 mM $MgSO_4$, 1 mM Na_4EDTA, 1 mM DTT, 10% (v/v) glycerol) plus 0.4 M NaCl (referred to as CytR Buffer elsewhere) was flash frozen in liquid nitrogen and stored in a nitrogen dewer.

Concentrations of these protein stocks were estimated by denaturing the proteins in 6 M GdmHCl and accounting for the absorbances of the denatured proteins from the extinction coefficients for amino acid residues (*17*, *18*) assuming additivity of absorbances. Referencing these concentrations back to the spectra of the native proteins yielded extinction coefficients at 280 nm of 18 400 M^{-1} for CRP and 8190 M^{-1} for CytR.

Construction of Gene Encoding CytR Core Domain. Two separate truncated CytR genes were designed to produce messages with AUG start codon immediately upstream of the codons for residues K63 and R64 of wild-type CytR. The Quik-Change PCR-directed mutagensis kit from Stratagene was used to convert the sequence immediately upstream of the K63 or R64 codon of the wild-type CytR gene carried by plasmid pCB091 to an NdeI site. Mutagenic primers (33 nt for K63 and 31 nt for R64) were purchased from Retrogen. In pCB091, the ATG start codon for full-length wild-type CytR is part of a unique NdeI site. Consequently, following the mutagenesis, the ca. 185 bp NdeI/NdeI fragment was removed by restriction digestion with NdeI and re-ligating the plasmid. A short NdeI/ClaI fragment (ca. 185 bp) was subcloned from each of the mutant plasmids into pCB091 to replace the 372 bp NdeI/ClaI fragment of the wild-type gene. The integrity of the mutant sequences was confirmed by dideoxy sequencing of the region subcloned. The truncated genes were isolated as 1.1 kb NdeI−BamH1 fragments and subcloned downstream of the T7 promoter carried by plasmid pSS584[2] to yield expression plasmids pNN001 and pNN002 for K63 and R64 Core domain, respectively.

Expression and Purification of CytR Core Domain. CytR Core domain was expressed using *E. coli* strain SS6142 transformed with either pNN001 or pNN002. Cells grown in Luria broth to mid to late log phase were induced to express Core domain by addition of 2% (w/v) lactose and 2

[2] pSS584 is a T7 expression plasmid that expresses genes from a translational frameshift. It contains a unique NdeI site as part of the frameshifted ribosome binding site downstream from the T7 transcription start site. SS6142 is a Tet^R, restriction negative, Trp^- T7 expression strain. pCB091 is a Kan^R, $NdeI^-$, $ClaI^-$, pBR322 derivative carrying the wild-type *cytR* allele. All are kind gifts from Steven A. Short (Molecular Sciences, Glaxo Welcome, Research Triangle Park, NC 274599).

mM IPTG. Core domain levels begin to plateau about 60−90 min after induction but continue to increase to at least 3 h. Core domain was purified from cells harvested 2.5 h post-induction.

Harvested cells were resuspended in 3.75 vol of Breaking Buffer (20 mM MOPS, pH_4 6.80, 0.3 M NaCl, 2 mM $MgSO_4$, 1 mM Na_4EDTA, 1 mM DTT) and lysed by one pass through a pre-cooled French Pressure cell at 12 000 psi. The protease inhibitor Pefabloc (4-(2-aminoethyl)benzene-sulfonyl flouride) and inhibitor cocktail Complete, both from Boehringer-Manheim, were added according to the manufacturer's recommendations to inhibit endogenous protease activity to which wild-type CytR is particularly sensitive (*11*). Centrifugation at 50 000 rpm and 4 °C for 3 h yielded cleared supernatant. Most soluble nucleic acid was precipitated by addition of polyethyleneimine to a final concentration of 0.02% (w/v). Precipitate was removed by low speed centrifugation (15 000 rpm and 4 °C for 20 min). The material that precipitated from the resulting supernatant at between 25 and 35% NH_4SO_4 was collected by low-speed centrifugation and dissolved in a small volume of CytR Buffer (see above) plus 0.3 M NaCl. Size-exclusion chromatography of this material was conducted on a Pharmacia HiLoad 16/60 Superdex 75 column equilibrated with CytR Buffer plus 0.3 M NaCl using an FPLC. Run conditions were 1.0−1.5 mL sample volume, 0.5 mL/min flow rate, and room temperature. Core domain elutes as the major peak at about 55 mL. Core domain containing fractions were pooled, and the NaCl was reduced to 0.15 M by dilution with salt-free CytR Buffer. This material was loaded onto 30 mL of Q-sepharose fast flow in a Pharmacia XK 16/20 column. The column was eluted with a 120 mL gradient from 0.15 to 0.5 M NaCl at a flow rate of 1 mL/min using an FPLC. Core domain elutes at about 0.3 M NaCl. Peak fractions were pooled and concentrated to about 5 g/L of Core domain. Purified protein was stored in this solution either at 4 °C or in a nitrogen dewer after flash freezing in liquid nitrogen.

The yield by this procedure is about 7−8 mg of protein per gram of wet cells. The purity, as assessed by SDS−PAGE, is 95−98%. In some cases, this purity was improved slightly by subsequent chromatography over a 30 mL S-sepharose fast flow column. Core domain loaded in CytR Buffer at 0.075 M NaCl elutes in the void volume.

The identity of the purified protein was confirmed by N-terminal protein sequencing and by MALDI-TOF mass spectrometry, both conducted by the Biomedical Protein Sequencing and MS Core Facility at the University of California, Irvine. Both techniques confirmed the presence of the N-terminal methionine, and neither detected any contaminating species. Core domain concentration was estimated spectrophotometrically using an extinction coefficient at 280 nm of 7400 M^{-1}. This was determined as described above for CytR and CRP. As for CytR, the lack of tryptophan in the structure accounts for the low extinction.

CytR Core Domain Activity. Determining the stoichiometry of cytidine binding assessed the fraction of active protein. With removal of the DNA-binding domain, this provides the only functional assay. The relative cytidine-binding stoichiometries of the different Core domain preparations used in these experiments were assessed using a nitrocellulose filterbinding assay. This was conducted as described previously (*4*) in a binding buffer composed of 10 mM bisTris (pH 7.00 ± 0.01), 100 mM NaCl, 0.5 mM $MgCl_2$, 0.5 mM $CaCl_2$, 1 mM dithiothreitol, and 100 μg/mL Ovalbumin. Binding reaction mixtures contained between 0.25 and 0.4 μM of either full-length CytR or Core domain dimer and 3−3.5 μM cytidine. Under these conditions, the K_d for cytidine binding to CytR and to Core domain are approximately 60 and 30 nM, respectively (see Results).

Since the nitrocellulose filters retain proteins with significantly less than 100% efficiency, this method can provide only relative estimates of CytR or Core domain fractional activity. The filterbinding results were calibrated by measuring the absolute cytidine binding stoichiometry for one Core domain preparation by using equilibrium dialysis. This indicated a lower limit of 96% activity for freshly prepared Core domain. By contrast, Core domain preparations had lost substantial activity (up to half) after several months of storage, and for these cases the cytidine-binding stoichiometry assay was used to normalize the concentration of active protein.

Filterbinding was also used for equilibrium measurements of cytidine binding to CytR and Core domain. Data were analyzed according to a simple Langmuir binding model such as given by eq 1. Protein concentrations in these experiments were 20−50 nM, a concentration that is similar to the K_d for cytidine. Consequently, the conservation polynomials for total cytidine and for total CytR (or Core domain) were solved for each data point and at each iteration of the nonlinear least-squares analysis of the binding data to calculate the free cytidine concentration.

Promoter DNA Preparation. A *udp*-containing DNA fragment was obtained from plasmid pCB039 (*4*). This plasmid contains the regulatory sequence of *udp* from 122 base pairs upstream from the transcription start site through the first 50 codons of *udp* (311 bp) cloned into the PstI and EcoR1 sites of pUC18. A 498 bp fragment containing this *udp* sequence was generated by restriction with PvuII and HindIII. A *deoP2* DNA fragment was obtained from plasmid pSS1332 (*4*). This plasmid contains the *deoP1P2* regulatory from −801 bp to +151 bp relative to the P2 start site cloned into pUC18. A 285 bp NotI/SmaI fragment containing just the *deoP2* sequence from −117 to +151 relative to the P2 start site was generated as described previously (*9*).

DNA fragments were purified by agarose gel electrophoresis from plasmids that were purified using the Qiagen EndoFree Plasmid kit. DNA was protein free, as judged by the UV spectrum. Fragments were labeled at their HindIII (*udp*) or NotI (*deoP2*) sites using the Klenow fill-in reaction as described (*9*) and purified using a Qiagen Nucleotide Removal kit. This generates labeled ends for footprinting experiments located approximately 25 and 35 base pairs upstream from the CRP2 sites of *deoP2* and of *udpP*, respectively.

Individual-Site Binding Experiments. Quantitative DNase I footprint titrations were conducted as described previously (*9*). The binding buffer used is similar to that described above for filterbinding assays but with Ovalbumin at 50 μg/mL and 1 μg/mL calf thymus DNA (CT-DNA) added. Experiments in which CRP was present also contained 150 μM cAMP, a concentration that maximizes the fraction of CRP present as the active DNA-binding species in which half of the cAMP sites are filled. CRP concentrations were corrected

Table 1: Configurations and Free Energy States for CRP and CytR Core Domain Association with *deoP2* and *udpP*

	Promoter Configuration[a]			free energy contributions[b]	free energy state
	CRP2	CytR	CRP1		
1	O	O	O	reference state	$\Delta G_{s,1}$
2	O	O	CRP	ΔG_1	$\Delta G_{s,2}$
3	CRP	O	O	ΔG_2	$\Delta G_{s,3}$
4	CRP	O	CRP	$\Delta G_1 + \Delta G_2$	$\Delta G_{s,4}$
5	CRP	Core domain	CRP	$\Delta G_1 + \Delta G_2 + \Delta G_{bridge}$	$\Delta G_{s,5}$
6	O	CytR	O	ΔG_3	$\Delta G_{s,6}$
7	O	CytR	CRP	$\Delta G_1 + \Delta G_3 + \Delta G_{13}$	$\Delta G_{s,7}$
8	CRP	CytR	O	$\Delta G_2 + \Delta G_3 + \Delta G_{23}$	$\Delta G_{s,8}$
9	CRP	CytR	CRP	$\Delta G_1 + \Delta G_2 + \Delta G_3 + \Delta G_{123}$	$\Delta G_{s,9}$

[a] Promoter configurations with sites denoted as filled (CRP, Core domain, or CytR) or empty (O). [b] The total Gibbs free energies of configurations 2−4 relative to the unliganded reference state (configuration 1) are given as a sum of free energy changes for intrinsic binding of CRP to CRP1 (ΔG_1) and to CRP2 (ΔG_2). Configuration 5 pertains to the complex formed by association of CytR Core domain in which ΔG_{bridge} represents the free energy change for bridging CytR−CRP interaction. Configurations 6−9 are shown for comparison. These pertain to cooperative promoter binding by full-length CytR. ΔG_3 denotes the free energy change for intrinsic binding of CytR to CytO. $\Delta G_{ij(k)}$ denotes cooperative free energy changes.

for this fraction, whose value is 0.64 ± 0.02 under the conditions employed (*9*).

Binding reaction mixtures (250 μL) were exposed to 5−8 ng of DNase I, added in a 5.0 μL vol, for 12.0 min and quenched by addition of 1/5 vol of 50 mM Na_4EDTA prior to addition of stop solution (*19*). Dried gels were imaged using a Molecular Dynamics Phosphorimager 435SI. Phosphor plates were exposed for 3−4 days and scanned at 176 μm spatial resolution. Analysis of the digital images was conducted using the program ImageQuant (Molecular Dynamics, Inc.) essentially as described (*20*, *21*).

The individual-site binding data were first analyzed separately for each site to obtain the Gibbs free energy change corresponding to K_{eq} ($\Delta G_i = -RT \ln K_{eq}$) in eq 1

$$\bar{Y}_i = P_o + (P_{max} - P_o)\left(\frac{e^{-\Delta G_i/RT}L}{1 + e^{-\Delta G_i/RT}L}\right) \quad (1)$$

Y_i is the fractional saturation of binding site i at the free protein ligand concentration, L. P_o and P_{max} are the baseline and maximum fractional protection for a given titration. For simple binding of either CRP or CytR alone, eq 1 gives the intrinsic free energy change for local binding, ΔG_i. For binding experiments in which both CRP and either CytR or Core domain are present, analysis according to eq 1 provides an accurate estimate of the individual site loading free energy change, $\Delta G_{l,i}$ and its confidence limits (*22*).

The free energy change for the association of CytR Core domain binding with the CRP_2−promoter complex (ΔG_{bridge}) was determined from paired experiments in which the promoter was titrated with CRP in the presence or absence of a fixed concentration of CytR Core domain (0.5−15 μM). Global analysis of the individual-site CRP binding data was conducted using equations that describe cooperative binding of CRP and Core domain according to the model defined by the promoter configurations listed in Table 1. Equations to describe CRP binding to CRP1 and to CRP2 were derived by considering the relative probability of each promoter configuration (f_s) as given by

$$f_s = \frac{e^{-\Delta G_s/RT}[CRP(cAMP)_1]^i[Core]^j}{\sum_{s,i} e^{-\Delta G_s/RT}[CRP(cAMP)_1]^i[Core]^j} \quad (2)$$

ΔG_s is the sum of free energy contributions for configuration s, (Table 1); i and j are the stoichiometries of bound CRP complexes (0, 1, or 2) and Core domain dimers (0 or 1) in configuration s. Summation of the relative probabilities for the configurations with protein bound to any given site yields the binding equation for that site. The model accounts for Core domain association only when CRP is bound to both CRP1 and CRP2.

Global numerical analysis was conducted as described (*23*) using the nonlinear least squares parameter estimation program, NONLN (*24*). Variances obtained from the initial separate analysis of each binding curve using eq 1 were used to calculate normalized weighting factors. Goodness and internal consistency of fits were evaluated based on two criteria: (i) comparison of the loading free energy changes for each of the individual sites in wild type and mutant operators as calculated from the global fitting parameters, to values experimentally determined; and (ii) comparison of the ratio of variances for separate and global analyses of binding to each individual site to the F statistic.

Mobility Shift Titrations. Mobility-shift titrations were conducted as described (*9*) using 3.5% acrylamide gels (29:1 acrylamide/BIS) and 0.5x TBE electrophoresis buffer (*25*). Proteins and *deoP2* DNA (1 nM of 285 bp fragment) were incubated 40−60 min at 20 °C (±0.1) in the DNase I footprint binding buffer plus 2 μg/mL CT-DNA and 1.5% Ficoll, which was added to facilitate gel loading. Aliquots (20 μL) of equilibrated binding reaction mixtures containing 500−600 dpm of ^{32}P were loaded onto 1.5 mm minigels in a BioRad Mini Protean II device that had been pre-electrophoresed for 5 min. Gels were electrophoresed at a constant 150 V for 35 min.

Dried gels were imaged as described above, and the images were analyzed as described (*9*, *26*) to determine the fraction of DNA in each electrophoretic band, Θ_i. Unliganded *deoP2* promoter DNA and the next three highest mobility bands were individually quantitated. Lower mobility bands are poorly resolved on the gel and so were grouped together to yield Θ_N. To analyze these data, each successive electrophoretic band was interpreted as representing *deoP2* DNA with one additional CRP dimer bound, without regard to the arrangement of filled and empty sites. This yields

$$\theta_i = e^{-\Delta G_{i,M}/RT}[CRP]^i / \sum_i (e^{-\Delta G_{i,M}/RT}[CRP]^i) \quad (3)$$

$\Delta G_{i,M}$ is the free energy change for binding of i CRP dimers to the unliganded *udp* promoter (i.e., related to the macroscopic product association equilibrium constant by $K_{i,M} = e^{-\Delta G_{i,M}/RT}$). The value of N in θ_N was treated as an adjustable parameter in the analysis, representing the average CRP stoichiometry of the higher order complexes.

Sedimentation Equilibrium Experiments. Proteins were equilibrated with 100 mM NaCl, 10 mM bisTris (pH 7.0), 0.5 mM $MgCl_2$, and 0.5 mM $CaCl_2$ by centrifugal buffer exchange using Bio-Spin 6 columns according to the vendor protocol. Sedimentation equilibrium experiments were con-

ducted at 20 °C in a Beckman XLA analytical ultracentrifuge using a 4-hole titanium rotor and either an 8-channel short column cell or an externally loaded 3-channel Yphantis cell, both with 12 mm thick Kel-F centerpieces and sapphire windows. Cells were loaded with 1:1, 1:2, 1:4, and 1:8 dilutions from initial concentrations of ~2−3 mg/mL for CRP; ~0.4 mg/mL for CytR; and 1:1, 1:3, and 1:9 dilutions of 2.7 mg/mL for Core domain. Mixtures of CRP and CytR were 1:1 and 1:3 dilutions of these initial concentrations.

Radial gradients of protein concentration were measured using Rayleigh interference optics. Data were collected at intervals after estimated time to equilibrium at each of four or five rotor speeds and tested for equilibrium by subtracting successive scans (*27*). Data within the optical window were selected using the program REEDIT (kindly provided by David Yphantis). These were analyzed using the program NONLIN (*28*) according to

$$C_r = \Delta C_j + \sum_N \exp\left[N\left(\ln C_{o,N} + \sigma\left(\frac{r^2}{2} - \frac{r_o^2}{2}\right)\right) + \ln K_N\right] \quad (4)$$

where C_r is the protein concentration (in fringe displacement units) observed at radial position r, ΔC_j is a baseline offset for channel j, $C_{o,N}$ is the concentration of species N at the meniscus (r_o), and K_N is the equilibrium association constant for formation of N-mers ($K_1 = 1$). The reduced molecular weight, σ, is given by $\sigma = M_r(1 - \bar{v}\rho)\omega^2/RT$ (*29*) where $\bar{v}$ is the partial specific volume, ρ is the buffer density, ω is the radial velocity, and R and T are the gas constant and absolute temperature, respectively. Conversion between reduced and nonreduced molecular weights used calculated buffer density, $\rho = 1.0025$ g/mL at 100 mM NaCl (*30*) and partial specific volumes, $\bar{v} = 0.7404$ L/g for CytR, $\bar{v} = 0.7453$ L/g for CRP, and $\bar{v} = 0.7404$ L/g for Core domain, calculated from the amino acid compositions (*31*).

In most cases, data were first analyzed using eq 1 by specifying a single molecular weight species ($N = 1$). When multiple species are present, this analysis yields a value close to the *z*-average of their molecular weight distribution (*32*). Subsequently, data from multiple channels obtained at different loading concentrations, radial positions, and angular velocities were analyzed by global nonlinear least squares to assess whether the protein dimers either self-associate to higher order oligomers or dissociate to monomers of. For this purpose, eq 1 was formulated to account for CytR, Core domain, or CRP dimers and for either or both monomers and higher order oligomeric species according to specified assembly schemes.

RESULTS

Design and Production of CytR Core Domain. Deletions of the N-terminal, DNA-binding domain of CytR were chosen to mimic the functional, ligand-binding Core domains that result from limited trypsinolysis of LacR (*33*) and PurR (*14*). CytR shares a conserved lysine residue in the hinge peptide that constitutes the preferred trypsin cleavage site for these other LacR family members (*3*). Trypsinolysis of CytR results almost exclusively in cleavage at this residue, K63, and the neighboring residue, R64; N-terminal sequencing indicated approximately an equimolar mixture of the two.

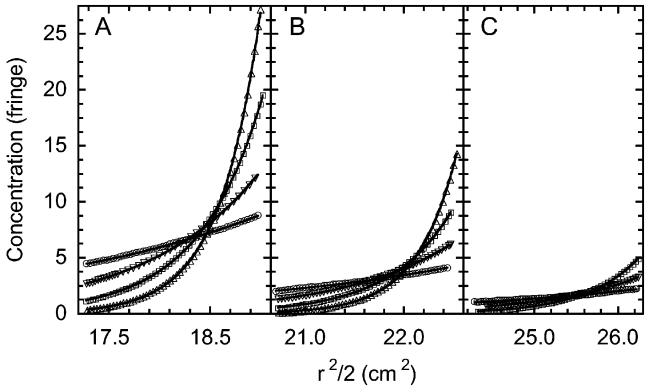

FIGURE 1: Sedimentation equilibrium analysis of CytRΔ2−63. The three channels of an Yphantis type cell were loaded with CytRΔ2−63 at 2.7 mg/mL (Panel A), 0.9 mg/mL (Panel B), and 0.3 mg/mL (Panel C) and centrifuged to equilibrium at speeds of 8000 rpm (circles), 12 000 rpm (down triangles), 16 000 rpm (squares), and 20 000 rpm (triangles). The buffer described for the DNA binding experiments was supplemented with 10% glycerol to stabilize the Core domain over the several days required for the experiment. Radial distributions are plotted as concentration vs one-half the square of the radius (one fringe equals 0.27 mg/mL). For clarity, only every seventh data point is shown. The solid curves represent the global analysis of these data according to eq 4, assuming a single molecular weight species. This yields $M_r = 58\,140 \pm 515$.

CytR Core domain isolated from tryptic digests binds cytidine with similar affinity as wild-type CytR (see below), indicating that these products of trypsin cleavage retain a stable structure. To obtain homogeneous preparations as necessary for biophysical analysis, genes were constructed to express two N-terminal deletions of CytR, CytRΔ2−62, and CytRΔ2−63. We refer generically to the proteins expressed from either of these genes and purified as described (see Materials and Methods) as CytR Core domain.

Self-Assembly and Binding Properties of Core Domain. The oligomeric state of CytRΔ2−63 was investigated by using sedimentation equilibrium. Radial distribution data were collected at three loading concentrations ranging from 0.3 to 2.8 mg/mL (10−90 μM in monomer) and four rotor speeds ranging from 8000 to 20 000 rpm (Figure 1). The radial concentration distributions obtained at different centrifuge speeds cross each other at a single point, and the concentrations of these crossover points reflect the loading concentrations of the three channels. This indicates no loss of the protein loaded because of aggregation and pelleting. The average molecular weight obtained by global analysis of these data using eq 1 was $58\,140 \pm 515$, or slightly less than expected based on the composition of CytRΔ2−63 dimer ($M_r = 62\,136$). The molecular weights obtained by analysis of individual radial distributions showed no systematic dependence on either rotor speed or loading concentration. Such dependence would be expected if there was significant dissociation to monomer or if a substantial population of other lower molecular weight contaminating species was present. Allowing for dissociation of dimer to monomer did not substantially improve the variance of the fit (<20%). No model that incorporates assembly of Core monomers to species larger than dimer gave an adequate fit to the data. These results suggest that CytR Core domain is homogeneous dimer in the μM concentration range, but do not eliminate the possibility of a very small fraction of lower molecular weight material (*27*).

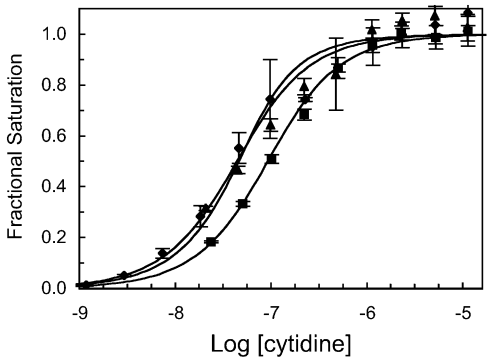

FIGURE 2: Filter binding assay comparing cytidine binding to wild-type CytR and CytR Core domain. Points plotted are averages (±standard deviations) of measurements on three separate equilibrium mixtures plotted vs total cytidine concentration for wild-type CytR (squares), CytRΔ2−62 (triangles), and CytRΔ2−63 (diamonds). The solid curves represent the analysis of these data as described in the text and accounting for the concentrations of both free and protein-bound cytidine. The difference in shape between the isotherms for CytRΔ2−62 and CytRΔ2−63 reflects different protein concentrations in the two experiments and the resulting effect on free vs total cytidine.

Cytidine Binding by Full-Length CytR and Core Domain. To assess whether deletion of the N-terminal, DNA-binding domain affects the functional properties of the allosteric Core domain, binding of the inducer ligand, cytidine was evaluated using a nitrocellulose filterbinding assay. Binding to both CytRΔ2−62 and CytRΔ2−63 was compared to binding by full-length CytR (Figure 2). Analysis of the data for wild-type CytR yielded $\Delta G = -9.6 \pm 0.1$ kcal/mol for binding of one cytidine per dimer as we showed to be the case previously (*4*). Results from matching titrations of CytRΔ2−62 and CytRΔ2−63 compare favorably: these yielded $\Delta G = -10.3 \pm 0.3$ kcal/mol and $\Delta G = -10.0 \pm 0.2$ kcal/mol, respectively. Indistinguishable results were also obtained for a mixture of CytRΔ2−62 and CytRΔ2−63 Core domain that was isolated from a limited trypsin digest of purified full-length wild-type CytR. These observations indicate that the cytidine-binding Core domain retains a nativelike structure when the DNA-binding domain is removed by trypsinolysis and also folds to form a nativelike structure when expressed as a truncated protein.

Electrophoretic Mobility Shift Analysis of Core Domain Association with the CRP_2−deoP2 Complex. We first employed a gel mobility shift assay to evaluate the interactions between the CytR Core domain constructs and the CRP_2−promoter complexes. Figure 3 presents typical results of experiments in which *deoP2* DNA was first titrated with CRP, and subsequently, CytRΔ2−63 was added. CRP binding in the absence of Core domain produced the expected pattern of mobility-shifted bands corresponding to species with either one or two CRP dimers bound. An additional band appearing at concentrations approaching μM CRP is consistent with nonspecific binding. Quantitative analysis of these data using eq 3 indicated sequential binding of CRP dimers to two sites of differing affinity. This is consistent with the pattern of energetics reported previously for CRP binding to CRP2 and CRP1 of *deoP2* (*9*) as well as other CytR-regulated promoters such as *udpP* (*11*), *nupG* (*12*), and *cdd* (*34*). The mobility shift experiments indicate approximately 3−4-fold lower affinity for CRP binding to CRP1 and to CRP2 (Figure 3) as compared to the results of

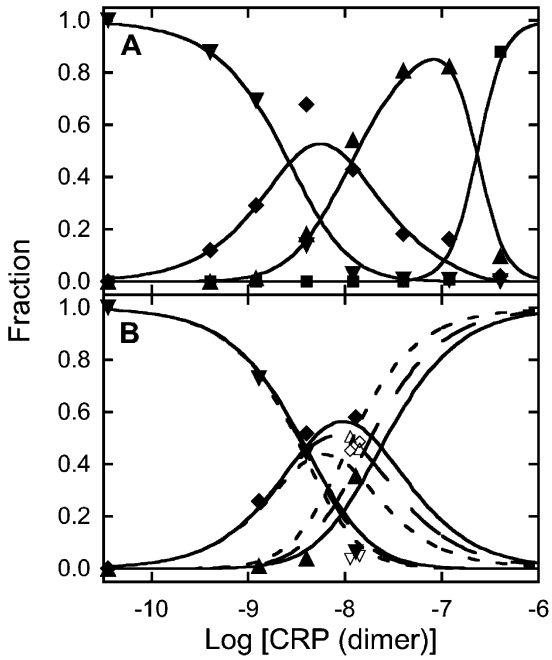

FIGURE 3: Gel mobility shift titration showing the effect of CytR Core domain on binding of CRP to *deoP2*. Panel A: CRP binding in the absence of CytR Core domain (CytRΔ2−63). Symbols represent θ_0, the fraction of DNA with no CRP bound (down triangles); θ_1, the fraction of DNA with one CRP dimer bound (diamonds); θ_2, the fraction of DNA with two CRP dimers bound (up triangles); and θ_N, the fraction of DNA with more than two CRP dimers bound as a result of nonspecific binding (squares). The solid curves represent analysis of these data using eq 3. The band representing nonspecific binding was modeled with a value of the stoichiometry, *N*, equal to 4. Converting the fitted values obtained for $\Delta G_{1,M}$ and $\Delta G_{2,M}$ into free energy changes for intrinsic, noncooperative binding of CRP yielded -10.9 ± 0.1 and -11.4 ± 0.1 kcal/mol for binding to CRP1 and to CRP2, respectively. Panel B: CRP binding but with CytR Core domain added to the reaction mixtures with the highest CRP concentrations (12.9 nM). The open symbols show systematic decreases in θ_0 and θ_1 and a systematic increase in θ_2 when CytR Core domain dimer is added at ca. 3.5 and 10 μM. These points are offset slightly in concentration for clarity. The solid curves fit the points obtained in the absence of CytR Core domain. The dashed lines are calculated to show the effect of addition of 3.5 μM (short dashes) and 10 μM (long dashes) CytR Core domain, assuming $\Delta G = -7$ kcal/mol for association of a Core domain dimer with the CRP_2−*deoP2* complex.

other assays such as quantitative DNase I footprinting (see below). It is not unusual to observe differences of this magnitude in comparing results from the two methods; this difference is similar as we have observed previously for CytR binding under the same conditions (*11*). We attribute this effect to dissociation of liganded complexes during gel loading and electrophoresis.

Figure 3 also shows the effect when CytRΔ2−63 was added to reaction mixtures containing CRP dimer at a concentration of 13 nM. At this concentration of CRP, the distribution of species is approximately 5% unliganded *deoP2*, 60% CRP_1−*deoP2*, and 35% CRP_2−*deoP2*. Addition of either 3 or 10 μM CytRΔ2−63 increased the fraction of CRP_2−*deoP2* and decreased both CRP_1−*deoP2* and to a lesser extent, unliganded *deoP2* (Figure 3B). This reflects an increase in apparent affinity for CRP binding when CytRΔ2−63 is present. Such an increase indicates cooperativity between Core domain and CRP for association with *deoP2*. In particular, CytRΔ2−63 results in net binding of

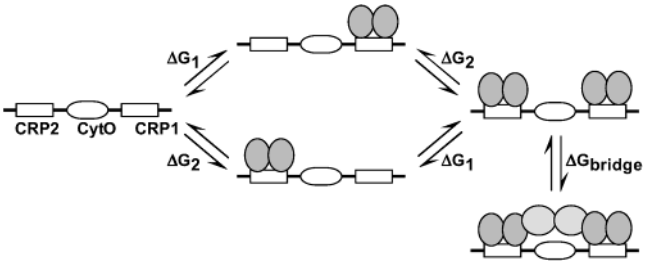

FIGURE 4: Linkage schematic indicating the macromolecular associations involved in formation of a bridged complex. ΔG_1 and ΔG_2 denote the free energy changes for intrinsic (and noncooperative) binding of CRP to CRP1 and CRP2, respectively. CytR Core domain associates when CRP is bound to both CRP1 and CRP2 as a result of favorably oriented protein−protein contacts, despite no interaction between Core domain and DNA. ΔG_{bridge} denotes the free energy change for this process. This model assumes no significant association of CytR Core domain when CRP is bound to either, but not both, CRP1 or CRP2.

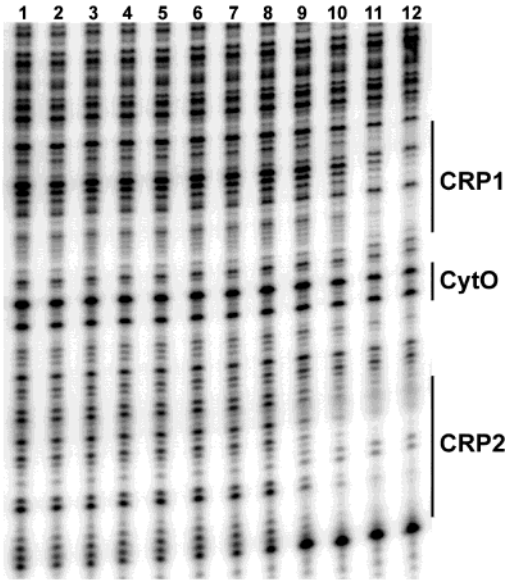

FIGURE 5: Footprint titration autoradiogram of CRP and CytR Core domain association with *deoP2*. Lanes 1−12 show promoter DNA being titrated with increasing concentrations of CRP dimer in the presence of 4.0 μM CytRΔ2−63 Core domain dimer. The fractional protection was determined for regions corresponding to sites CRP1 and CRP2 as indicated in the figure. Weak protection is also evident in the region flanked by these sites as a function of increasing CRP concentration. The region used to analyze this protection is indicated. These analyses generated the data plotted in panel B of Figure 6, below.

the second CRP dimer. This indicates an interaction between CytRΔ2−63 and both DNA-bound CRP dimers, which is consistent with formation of a bridged complex.

Formation of the bridged complex did not produce a separate supershifted electrophoretic band under the conditions employed. However, the consistency with which we observed similar changes in the populations of the intermediate species when Core domain was added provides confidence that the bridge complex does form. Therefore, either complexes with and without CytRΔ2−63 are not resolved electrophoretically under these conditions or CytRΔ2−63 does not remain associated throughout the electrophoresis. The changes in populations proved to be too small to yield precise estimates of ΔG for Core domain association. But as a preview to results obtained using a more definitive approach (see below), we have plotted curves (Figure 3) that

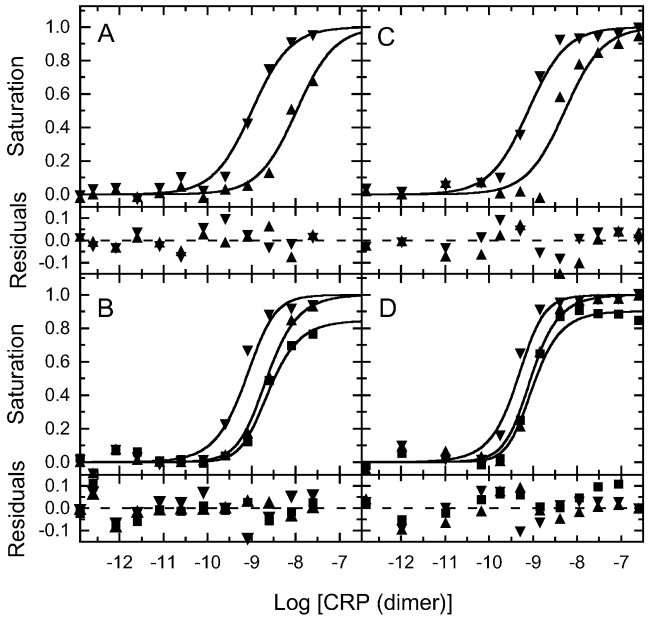

FIGURE 6: Effect of CytR Core domain on binding of CRP to the *deoP2* and *udp* promoters. Individual-site binding isotherms were generated by footprint titration of CRP binding in the presence (panels B and D) and absence (panels A and C) of fixed concentrations of CytR Core domain. Panels A and B represent paired titrations to show the effect of 4.0 μM CytRΔ2−63 Core domain dimer on CRP binding to *udpP*; panels C and D represent paired titrations to show the effect of 13.1 μM CytRΔ2−63 Core domain dimer on CRP binding to *deoP2*. Symbols denote the different operator sites: upward triangles, CRP1; downward triangles, CRP2; and squares, Core domain bridging. The curves represent global analysis of each pair of titrations according to the model shown in Figure 4. Residuals from these fits are shown below each panel.

represent the predicted populations of intermediates in the presence of 3 or 10 μM Core domain if $\Delta G \approx -7$ kcal/mol for association of Core domain with CRP_2−*deoP2*. The quantitative agreement between predicted and observed intermediate populations is quite reasonable. Whereas −7 kcal/mol is a large free energy change as compared to the heterologous cooperativity exhibited when full-length CytR binds to CRP_2−*deoP2* ($\Delta G \approx -2.5$ to −3 kcal/mol (*9*, *11*)), it indicates a very low affinity for analysis by gel-shift assay. Consequently, it would not be surprising if Core domain dissociates during electrophoresis.

Analysis of Bridging Interaction by DNase I Footprinting. Following the lead provided by the electrophoretic mobility-shift results, we evaluated Core domain binding to the CRP_2−*deoP2* and CRP_2−*udpP* complexes by considering the thermodynamic linkage between this reaction and binding of CRP to CRP1 and CRP2, as depicted in Figure 4. ΔG_{bridge} denotes the free energy change for Core domain binding to the CRP_2−promoter complex to form the bridged complex. Since this association favors promoter complexes with two CRP dimers bound, thus mimicking cooperative CRP binding, ΔG_{bridge} can be evaluated by comparing CRP binding in the presence and absence of fixed concentrations of CytR Core domain.

Figure 5 presents a footprint autoradiogram from a representative experiment in which *deoP2* was titrated with CRP in the presence of 4.0 μM CytRΔ2−62 dimer. Increasing protection from DNase I mediated cleavage is observed as the CRP concentration is increased, indicating site-specific

binding of CRP. The fractional protection was quantitated separately for regions corresponding to CRP1 and to CRP2, as indicated in the figure to generate data presented in Figure 6. Figure 6 depicts CRP binding to *deoP2* in the presence and absence of 4.0 μM CytRΔ2−62 dimer (left-hand panels) and 13.1 μM CytRΔ2−63 dimer (right-hand panels). Comparing top and bottom panels, the stabilization that results from Core domain bridging is evident in the leftward shift of the CRP1 binding isotherms, and the apparent cooperative effect is evident in the sharper transitions for CRP binding to both sites. As expected, the stabilization resulting from the association of CytR Core domain is more acute for CRP1 as a consequence of its lower intrinsic affinity for CRP binding (*35*).

In addition, a sequence of DNA located between CRP1 and CRP2 shows weak protection from DNase I mediated cleavage in the presence of Core domain (Figure 5) but not in its absence. Control experiments confirmed that this protection requires the presence of CRP; no protection was observed in the absence of CRP, even at a concentration of Core domain of 48 μM. The degree of protection upon saturation by CRP is less than at the CRP sites (e.g., only about 50%). This indicates significant exposure to DNase I even in the bound complex. Analysis of this protection produced the third set of points (square symbols) shown in the bottom panels.

We interpret this additional protection as reflecting bridged complex formation, which offers the underlying DNA partial protection form DNase I mediated cleavage even in the absence of direct physical contact between CytR Core domain and DNA. Consistent with the interpretation that this reflects saturable binding of CytR Core domain, the extent of protection decreases with decreasing concentration of Core domain. For example, the maximum fractional protection when both CRP sites are filled is above 80% in panels B and D, for which Core domain concentrations are 4.0 and 14.5 μM, respectively. In contrast, at the lowest Core domain concentration at which bridge complex formation was detectable by its effect on CRP binding (0.5 μM Core domain), protection of the DNA between CRP1 and CRP2 could not be discerned above the background.

Global analysis of the protection at CRP1 and CRP2 was conducted according to the model comprised of configurations 1−5 listed in Table 1, using eq 2. Separate analysis of the data generated using CytRΔ2−62 (panels A and B) and CytRΔ2−63 (panels C and D) yielded similar estimates of ΔG_{bridge}. The results are shown as the curves drawn through the points for these sites. The curves showing the protection generated by Core domain bridging in panels B and D were also calculated using the parameters obtained from these fits. Since these data were not included in the fitting, the close correspondence between the predicted binding isotherms and the protection observed provides strong support for our interpretation that this protection results from the association of Core domain to form the bridged complex.

Results of an extensive series of similar experiments conducted on both *udpP* and *deoP2* are presented in Table 2. These tabulated values confirm no difference in bridging behavior between CytRΔ2−62 and CytRΔ2−63. This obviates potential concerns that the structure of the Core domain and its interactions with promoter-bound CRP might be sensitive to the particular N-terminus. These results also establish that ΔG_{bridge} is the same for association of CytR Core domain with *udpP* as with *deoP2*.

Table 2: Free Energy Changes for Formation of CRP−CytR−CRP Bridged Complex on Operator DNA[a]

operator	Core domain	ΔG_2	ΔG_{bridge}	ΔG_1
udpP	K63	−12.9 ± 0.2	−7.8 ± 0.2	−11.2 ± 0.2
udpP	R64	−12.6 ± 0.6	−7.8 ± 0.5	−11.5 ± 0.5
deoP2	K63	−12.1 ± 0.2	−7.5 ± 0.5	−10.7 ± 0.3
deoP2	R64	−12.2 ± 0.2	−7.9 ± 0.3	−11.0 ± 0.2

[a] Free energy changes for intrinsic binding of CRP to operator sites CRP1 and CRP2 of the *E. coli udp* and *deoP2* promoters and for subsequent binding of CytR Core domain to form the DNA-bound CRP−Core domain−CRP bridged complex. These were obtained by global analysis of matched CRP titrations conducted in the presence and in the absence of fixed concentrations of Core domain dimer, as shown in Figure 4. CytR Core domain dimer concentrations used in individual experiments ranged from 0.5 to 14.5 μM. Values of ΔG^o shown (units of kcal/mol) are means of multiple determinations (±SD of the mean).

An additional experiment was conducted to investigate directly the association of CytRΔ2−63 to form a bridged complex with CRP_2−*deoP2*. *DeoP2* was titrated by CytRΔ2−63 at a fixed concentration of CRP dimer (45 nM) sufficient to nearly saturate both CRP1 (82%) and CRP2 (96%). The protection generated by Core domain bridging was analyzed according to a simple Langmuir model (eq 1) for Core domain binding, which reflects the equilibrium shown vertically in Figure 4. The results of this direct titration yielded $\Delta G_{bridge} = -7.4 \pm 0.1$ kcal/mol in good agreement with the results obtained indirectly by analysis of CRP binding (Table 2). The average of this value plus each of the individual estimates (eight) represented in Table 2 yields $\Delta G_{bridge} = -7.8 \pm 0.2$ kcal/mol, which corresponds to an equilibrium dissociation constant, $K_d = 1.4$ (within a factor of 1.5) μM, for association of CytR Core domain with a CRP_2−promoter complex.

Effect of Cytidine Binding to CytR on CytR Bridging. Next we assessed whether bridge complex formation is coupled to cytidine binding by CytR. To address this question experimentally, matched CRP binding titrations of both *deoP2* and *udpP* were conducted with and without CytR Core domain, as before (Figure 6), but now also comparing the presence and absence of 1 mM cytidine. At this concentration, CytR Core domain is over 99.99% saturated with cytidine (see above). Results for *deoP2* are presented in Figure 7. Analysis of these experiments and of similar titrations of *deoP2* yielded $\Delta G_{bridge} = -7.9 \pm 0.4$ kcal/mol in the absence of cytidine, in excellent agreement with results cited above.

The influence of cytidine is apparent from the reduced fractional protection of CytO at saturating CRP (Figure 7). Protection is nearly eliminated at this concentration of CytRΔ2−63, indicating significantly lower affinity for association with CRP_2−*deoP2* to form the bridged complex. As before, an estimate of ΔG_{bridge} can be obtained based on its effect on CRP binding. Global analysis of the individual site binding isotherms for CRP1 and CRP2 yielded −5.9 kcal/mol for cytidine-liganded CytRΔ2−63, with a high affinity limit of −6.8 kcal/mol. This indicates that cytidine binding to CytR and bridging of CytR between pairs of DNA-bound CRP dimers are thermodynamically coupled

Table 3: Sedimentation Equilibrium Analysis of CytR and CRP[a]

protein	effector ligand[b]	concentrated[c] (μM)	speed[d] (rpm × 10^3)	$M_{z,app}$[e] (× 10^3)	s[f]
CytR		5	20, 26, 32, 36, 40	73.9 (70.3, 77.6)	0.021
CytR	cAMP cytidine	5	20, 25, 30, 35, 40	69.3 (65.5, 73.7)	0.032
CRP	cAMP	40	15, 24, 30, 35, 40	44.1 (43.0, 45.3)[g]	0.021
CRP		40	15, 24, 30, 36, 40	43.0 (41.2, 44.3)	0.026

[a] Serial dilutions of CytR (0.4 mg/mL) and CRP (2.3 mg/mL) were loaded into 8-channel, short column cells and centrifuged to equilibrium at rotor speeds indicated. [b] Effector ligand concentrations are 150 μM cAMP and 1.00 mM cytidine. [c] Maximum observed protein concentration in μM dimer, as determined by cross-over point analysis of scans from successive speeds. [d] Rotor speeds used for data collection. [e] M_r obtained by global analysis of data acquired at all protein dilutions and rotor speeds when data were fitted using eq 4 assuming a single species. This analysis yields a molecular weight similar to the z-average when multiple species are present. 95% confidence limits are in parentheses. [f] Square root of the variance in units of Rayleigh fringe displacement.

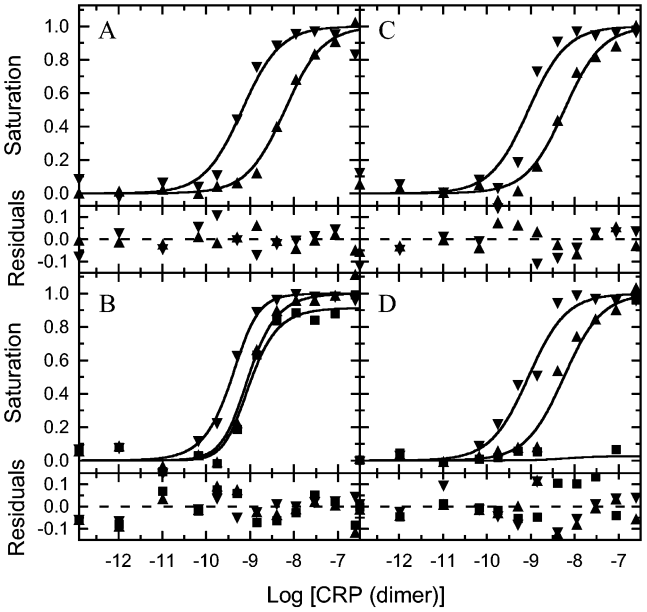

FIGURE 7: Effect of cytidine on bridged complex formation. Parallel experiments of individual-site binding of CRP to the *deoP2* promoter in the presence (panels B and D) and absence (panels A and C) of 13.1 μM CytRΔ2−63. Cytidine was present at 1 mM concentration in the titrations shown in panels C and D. Symbols denote the different operator sites as in Figure 6: upward triangles, CRP1; downward triangles, CRP2; and squares, Core domain bridging. The curves were drawn according to the model shown in Figure 4 with $\Delta G_{bridge} = -7.9$ kcal/mol in the absence of cytidine and $\Delta G_{bridge} = -4.5$ kcal/mol in its presence, as described in the text. Residuals from these fits are shown below each panel.

processes. Significantly, these are the same value and limit that were obtained from analysis of titration data for *udpP*. This indicates that the coupling is thermodynamically similar at these promoters. However, with so little bridged complex formed at these CytRΔ2−63 concentrations (13−15 μM), the stabilizing effect on CRP binding is small, and a lower affinity limit for CytRΔ2−63 association is not precisely determined. Sufficient concentration of CytRΔ2−63 to evaluate the lower bound in this manner is currently not technically achievable.

As an alternative, CRP_2−*deoP2* was titrated directly by CytRΔ2−63 as described earlier but in the presence of 1.0 mM cytidine. At the highest CytRΔ2−63 concentration attained (48.4 μM), the maximum protection achieved in the footprint experiment was approximately 0.08 corresponding to a similarly low fractional occupancy by CytRΔ2−63. To analyze these data, the fractional protection at saturating CytRΔ2−63 (P_{max} in eq 1) was estimated by conducting a parallel titration experiment in the absence of cytidine so that saturation was achieved. This analysis provided a well-bounded value, $\Delta G_{bridge} = -4.5 \pm 0.3$ kcal/mol, for cytidine-liganded Core domain. The solid curves drawn though the data in Figure 7 reflect this value. The fitted value of $P_{max} = 0.94 \pm 0.05$ is near its physical limit of 1. Given the numerical correlation between ΔG_{bridge} and P_{max}, this defines −4.5 kcal/mol as an absolute lower limit to the affinity for association of cytidine-liganded Core domain.

Solution Assembly of CytR and CRP. Sedimentation equilibrium analysis was employed to investigate the association between free CytR and free CRP. The fact that CytR Core domain associates to form a bridged complex confirms that such protein−protein interactions underlie cooperative DNA binding. On the basis of $\Delta G_{bridge} \approx -8$ kcal/mol, ΔG of the order −3 to −4 kcal/mol might be anticipated for a 1:1 association between CytR and CRP to form a hetero-tetrameric complex. This corresponds to a k_d for tetramer to dimer dissociation in the 1 mM range, or at the edge of detection, whether by sedimentation equilibrium or other experimental technique.

Results of sedimentation equilibrium experiments conducted on each protein alone are summarized in Tables 3. Experiments were conducted both in the absence and in the presence of saturating concentrations of effector ligands, cAMP and cytidine. Results for full-length CytR at multiple speeds and loading concentrations differed from what was obtained for CytR Core domain (CytRΔ2−63; see above) in that the crossover points between radial distributions at successive centrifuge speeds moved systematically toward higher radial positions. This indicates loss of material at higher loading concentrations such as would result from precipitation. The behavior was observed to be speed dependent, but not time dependent. This suggests reversible precipitation of CytR as the solubility limit is reached, rather than an irreversible process such as denaturation-linked aggregation. Analysis of the crossover concentrations between successive scans (*36*) indicated average channel concentrations corresponding to the solubility limit of approximately 5 μM in CytR dimer (0.4 g/L).

Global analysis of these data indicates that CytR is dimeric in solution, as expected. Analysis according to a model accounting for a single species (Table 3) yielded molecular weights similar to but slightly less than as calculated for CytR dimer (75 640) from its composition. As with the analysis of CytR Core domain (CytRΔ2−63), a model accounting for dimer dissociation could not be fitted suggesting that these slightly lower molecular weights result from a small percentage of nonassociating monomer (*27*). The similarity

Table 4: Sedimentation Equilibrium Analysis of CytR−CRP Mixture[a]

		Single Species[d]	Monomer−dimer Association[e]		
effector ligand[b]	speed[c] (rpm × 10^3)	$M_{z,app}$ (× 10^3)	M_2[f] (× 10^3)	ΔG^o_{2-4}[g] (kcal/mol)	s[h]
cAMP	15, 26, 32, 36, 40	52.7 (49.7, 55.8)[g]	48.4 (47.5, 49.9)	−3.94 (−3.91, −4.12)	0.045
cAMP cytidine	20, 26, 30, 32, 36, 40	51.6 (49.7, 53.4)	48.6 (47.5, 49.9)	−3.70 (−3.66, −4.12)	0.036

[a] Serial dilutions of a mixture containing CytR (0.4 mg/mL) and CRP (2.3 mg/mL) were centrifuged to equilibrium at speeds indicated. [b] Effector ligand concentrations are 150 μM cAMP and 1.00 mM cytidine. [c] Rotor speeds used for data collection. [d] M_r obtained by global analysis of data acquired at all rotor speeds when data were fitted using eq 1 assuming a single species. 95% confidence limits are in parentheses. [e] Parameter values obtained by global analysis of data acquired at all rotor speeds when data were fitted using eq 1 assuming self-assembly of a single average dimeric species to form a tetramer. Values in parentheses are 95% confidence limits. [f] M_r obtained for the dimeric species. [g] Gibbs free energy change in kcal/mol for association. [h] Square root of the variance in units of Rayleigh fringe displacement.

between what was observed for Core domain and full-length CytR suggests as another possibility to explain some of the difference between observed and expected molecular weights that the calculation of $\bar{v}$ from the amino acid composition might not be accurate in this case. Models accounting for higher-order oligomerization (tetramers and above) were also investigated. These did not improve the fit and yielded k_d values for higher-order assembly corresponding to affinities in the mM range. These values are substantially beyond the solubility limit for CytR and as such are outside the range of reliable detection.

Consistent with previous findings *(9)*, sedimentation equilibrium analysis also indicates that CRP is primarily dimeric (Table 3). Global analysis of radial distributions corresponding to multiple speeds and loading concentrations yielded molecular weights slightly less than what is calculated based on the composition (46 966). Fitting the data using assembly models that account for higher-order oligomers did little to improve the fit, and as for CytR, yielded k_d values outside the range of reliable estimation.

Results of sedimentation equilibrium experiments conducted on a mixture of CytR and CRP are summarized in Table 4. Initial concentrations were approximately 5.2 CytR dimer and 52 μM CRP dimer. Given the relatively low solubility limit for CytR, a high CRP concentration was used to drive the assembly and maximize sensitivity to hetero-oligomers. Experiments were conducted in the presence of 150 μM cAMP, a concentration that maximizes the proportion of the active CRP species in which cAMP is bound to only the low affinity cAMP sites (*9*, *37*). Experiments were conducted in the absence and presence of saturating cytidine (1 mM). The radial distributions from all rotor speeds and loading concentrations were first analyzed globally using eq 1 accounting for only a single species to estimate the *z*-average molecular weight of species present. This yielded $M_{z,app} \approx 52$ kDa (Table 4), which is similar to that calculated for a nonassociating mixture of the two homodimers at their initial concentrations (49.9 kDa). Notably, the same estimate of $M_{z,app}$ was obtained when cytidine was present.

Subsequently, the data were analyzed according to the model accounting for a dimer-tetramer self-association. This analysis also yielded identical results in the presence and absence of cytidine. In both cases, the fitted dimer molecular weight was consistent with the *z*-average molecular weight of the mixture of the two homodimers. This indicates that the model is a fair approximation to the heteromeric association of CytR and CRP to form tetramers. The free energy change for the association reaction (Table 4) is consistent with a k_d for hetero-tetramers of 1 mM. This corresponds to about 4% of the CytR assembled as hetero-tetramer at the loading concentrations used. As expected, accounting for such a small fraction of an additional species has only a small effect on the variance of the fit. This indicates that the value is beyond the limit of reliable estimation by this method.

Sedimentation velocity experiments were also conducted on the mixture of the two proteins, and these confirmed the results of the sedimentation equilibrium experiments. Two overlapping peaks were observed whose sedimentation values correspond to what was determined separately for the individual proteins ($s_{20,w} = 3.5$ for CRP and 4.5 for CytR). There was no evidence for higher-order assemblies at the concentrations used in these experiments. We would not expect to detect a 4% population of CytR−CRP hetero-tetramer but can be confident that appreciably higher levels are not present.

DISCUSSION

With only two regulatory proteins, the CytR regulon presents a relatively simple example of combinatorial gene regulation and therefore an exceptional opportunity for a complete understanding of this process in molecular terms. Despite the simplicity of components, the differential regulation of unlinked genes is fairly sophisticated. CRP is known to be capable of directing multiple mechanisms of activation from different regulatory sites (*7*) as are found in CytR-regulated promoters. Although it binds to only one primary operator, CytR appears to direct more than one mechanism of repression (*6*). Different combinations of these multiple mechanisms of activation and repression are thought to account for differential regulation.

Cooperative binding of CytR and CRP is a critical component of both repression and induction. At both *deoP2* and *udpP*, promoters that have been extensively analyzed quantitatively (*9*−*11*), cytidine binding by CytR reduces cooperativity. Since protein−protein association is thought to provide the driving force for cooperativity in most cases, a reasonable expectation is that cytidine binding to CytR would be coupled directly to CytR−CRP association. But this simple explanation is contradicted by the observation that cytidine binding has different qualitative effects on cooperativity at these two promoters (*11*). The correlation between the difference in response to cytidine and the different regulatory properties of these two promoters implicates the linkage between cytidine binding and cooperativity as an important component of the differential control. But if cytidine binding is not coupled directly to

CytR−CRP association, then how does it modulate cooperativity, and what accounts for different effects in different promoters?

The product of protein−protein association is always an oligomeric complex with the possibility to make simultaneous interactions with multiple DNA sites. In this situation, the first interaction anchors the protein complex in the proximity of the additional sites, which by itself tends to increase the probability of additional interactions, thereby contributing favorably to cooperativity. Conversely, the association between DNA-bound proteins can be more favorable than association between the free proteins in solution because of their proximity when DNA-bound. This is equivalent to a high local concentration of these reactants. In energetic terms, if most of the loss of translational, vibrational, and rotational energy that accompanies macromolecular association is paid by the first interaction, the result can be a free energy change for binding of an oligomer, such as CytR−CRP heterotetramer, that is more favorable than the sum of free energy changes for separate binding of the individual proteins. The difference between the free energy change for simultaneous interaction and the sum of free energy changes for the individual interactions has been denoted as the connection free energy, $\Delta G^{o}_{connect}$ (*38*). This is related to the effective local concentration (C_{eff}) according to the usual thermodynamic relationship, $\Delta G^{o}_{connect} = -RT \ln C_{eff}$.

But this advantage for association between DNA-bound proteins disappears if the structure of the oligomeric protein complex does not conform to the spacing and/or helical orientation of DNA-binding sites. In that case, association of DNA-bound proteins, or conversely, simultaneous binding of an oligomeric complex, requires conformational adaptation of one or both macromolecules, DNA (e.g., bending and twisting), and protein complex. This must contribute unfavorably to the connection free energy. In this way, the promoter can play a critical scaffolding role to control the higher-order protein associations that govern the functional states of transcription regulatory assemblies. Allosteric mechanisms can also contribute to the connection free energy. This is the case if different molecular interactions (e.g., protein oligomerization, intrinsic DNA binding, and binding of an effector ligand such as cytidine) are thermodynamically linked. This can contribute to $\Delta G^{o}_{connect}$ either favorably or unfavorably.

We, as well as others, have shown a variable balance of these energetic contributions in different gene regulatory systems (*26*). It is common for cooperative free energy change to be less favorable than the free energy change for protein−protein association. This indicates a positive $\Delta G^{o}_{connect}$. We inferred that this must be the case for CytR-regulated promoters, as outlined in the introductory section and supported by the data we present here. The connection free energy provides a convenient framework for dissecting the cooperative free energy into the component contributions from different macromolecular processes. To assess these effects and their linkage to cytidine binding, we investigated the assembly of CytR and CRP in solution and compared this to the association of the Core domain dimer with tandem, promoter-bound CRP.

Results of the sedimentation analysis indicate only weak association, if any, between CytR and CRP dimers in solution. When analyzed rigorously, using a heteromeric assembly model in eq 4, the parameter values were too highly correlated for the fit to converge. Consequently, the data were analyzed assuming self-association as an approximation. When analyzed in this manner, the monomer molecular weight obtained as a fitting parameter was consistent with the *z*-average molecular weight of the mixture of CRP and CytR homodimers as described earlier. In this model, the association of the *z*-average molecular weight monomer corresponds to assocation of CytR and CRP. The ΔG obtained for this reaction accounts for only a small fraction of CytR and CRP dimers associated as a tetramer. When the association is weak, as it is here, the self-association model is a good numerical approximation of the actual heteromeric assembly.

ΔG values as obtained from this analysis are tightly bounded, both for the association of CRP with free CytR and with cytidine-liganded CytR (Table 4). The values rule out an affinity for assembly greater than approximately 1 mM. We note that even such weak assembly could account for the cooperativity since ΔG for pairwise cooperativity is only about −1.4 kcal/mol (*9*, *11*). Despite the narrow confidence intervals obtained in the fit, the data do not eliminate the possibility of affinity weaker than 1 mM. Even a small quantity of aggregated material could account for the apparent higher molecular weight species in the analysis. However, even at 1 mM, the affinity for association is unexpectedly low. Such low affinity leaves little room to provide specificity of interaction. On the basis of this reasoning, it is significant that the same parameter values were obtained in the presence and absence of saturating cytidine. This observation is consistent with the conclusion that cytidine binding to CytR does not effect CytR−CRP association.

If cytidine does not affect CytR−CRP association per se, then does it affect simultaneous interaction of CytR with two CRP dimers to form a protein−protein bridge? To address this question requires CytR Core domain in which the interaction between CytR and DNA is eliminated but other CytR functions (i.e., dimerization, cytidine binding, and CRP association) are unperturbed. Three observations instill confidence that this is the case for the Core domain constructs we have expressed and purified, as it is for homologous LacR family proteins. First, both proteins are tight dimers, similar to full-length CytR. This observation is consistent with the expectation that the dimer interface is contained entirely within the Core domain (*39*). Second, cytidine binding by Core domain and full-length CytR is similar. Third, the two Core domain constructs give identical results with respect to both self-association and ligand binding, indicating no effect of the precise location of the truncation. In addition, neither protein associates with promoter DNA to a detectable extent in the absence of CRP binding.[3] Thus, we believe that the results obtained with these proteins reflect accurately

[3] The first experimental evidence to suggest CytR bridging was obtained using another deletion mutant, CytRΔ9−48 (*13*). Data reported for this mutant suggested a surprisingly high affinity of ca. 1−3 nM under the low salt conditions used in the experiments. This is a similar affinity as for cooperative binding of full-length CytR (*9*, *11*). This mutant retains the lysine-rich N-terminal nine residues of CytR, capping a 14-residue hinge peptide that is thought to be largely unstructured (*40*). This peptide represents a plausible ligand for nonspecific interaction with DNA (cf., ref *41* and refs therein). Consistent with this explanation, deletion of this lysine-rich sequence led to considerable loss of repressor activity (*13*).

the energetic contribution that results from interaction between full-length CytR and CRP.

In contrast to the low affinity for solution assembly of CytR and CRP, these two CytR Core domain constructs show appreciable affinity for bridging between tandem, DNA-bound CRP dimers. The free energy change we obtain for this interaction, $\Delta G^{o}_{bridge} = -7.8$ kcal/mol, is essentially double what we estimate for solution assembly of CytR and CRP to form a heterotetramer. This suggests that the separate interactions between CytR and each CRP dimer are additive, yielding a connection free energy of zero for bridging. Whatever advantage is afforded by arranging the CRPs as bound to promoter DNA must be countered by some other contribution to $\Delta G^{o}_{connect}$. We also note that ΔG^{o}_{bridge} is the same for *deoP2* as for *udpP*. The distance bridged in these two complexes differs by only one bp; evidently, the bridged complex has the flexibility to accommodate the slight difference expected in distance and rotational orientation.

On the basis of this value for ΔG^{o}_{bridge}, the connection free energy that pertains to the cooperatively bound complex in which CytR both bridges between tandem DNA-bound CRP dimers and also binds CytO is easily calculated. Summing ΔG^{o}_{bridge} (−7.8 kcal/mol) and the free energy change for intrinsic binding of CytR to CytO of either *deoP2* (−10.4 kcal/mol; ref *9*) or *udpP* (−10.7 kcal/mol; ref *11*) and subtracting the free energy change for cooperative binding of CytR to these promoters (−13.1 and −12.9 kcal/mol, respectively) yields $\Delta G^{o}_{connect} \approx +5$ kcal/mol. The value of $\Delta G^{o}_{connect}$ yields $C_{eff} \approx 0.2$ mM. Therefore, at the standard state of 1 M, the effective concentration of CytR bound to CytO is 4 orders of magnitude less than free CytR. We conclude that the interactions CytR makes with CRP and those it makes with the promoter DNA are highly antagonistic.

One potential source of unfavorable contribution to $\Delta G^{o}_{connect}$ is from DNA bending in forming a cooperatively bound, CRP−CytR−CRP complex. For CytR to bridge the gap between promoter-bound CRP dimers and juxtapose the interacting surfaces of CytR and CRP as delineated by mutagenesis experiments (*39*), the promoter DNA must be bent substantially. For example, in a three-dimensional model of the complex constructed by Valentin-Hansen and colleagues (*39*), 70 bp of promoter DNA circumscribes an arc of about 90°, an energetically unfavorable conformation. Of course, the promoter DNA must also bend to form the bridged complex and this might explain why the connection free energy for this process is unfavorable. However, the additional interaction between CytR and CytO in the cooperative complex must place additional constraints on the conformation of the promoter DNA, constraints that would contribute to the large positive $\Delta G^{o}_{connect}$ for this process.

Interesting in this regard are results of SELEX experiments (*42*). These implicate both a preferred spacing of 11 bp between the recognition half-sites of CytO and also a preferred centro-symmetric arrangement of operator sites in which CytO is located midway between CRP1 and CRP2 in the cooperative complex. The modeled structure of the complex conforms to these preferences resulting in a conformation in which the DNA is curved uniformly along its length. However, neither the spacing nor arrangement of operators in this model conforms to any of CytR-regulated promoters.

The SELEX experiments also indicate a different preference of CytR for the spacing between CytO half-sites depending on whether CytR binds alone or as a component of the cooperatively bound complex (*42*). This fact suggests that binding to DNA and associations with CRP are coupled structurally. If this were accompanied by thermodynamic linkage, as seems certain, it would also contribute to $\Delta G^{o}_{connect}$. A direct way to evaluate the linkage would be to compare association of operator-oligonucleotide-bound CRP and CytR to association of free CRP and CytR (*26*, *43*). Unfortunately, this approach is not feasible in this case because of the low affinity for CytR−CRP association.

Cytidine binding results in a substantial decrease in the stability of the bridged complex. Our results indicate a reduction in ΔG^{o}_{bridge} from −7.8 kcal/mol for unliganded Core domain to −5.9 kcal/mol (limits of −6.8 to −4.5 kcal/mol). This reduction in ΔG^{o}_{bridge} is by itself approximately sufficient to account for the nearly complete loss of cooperativity in the three-protein, CRP−CytR−CRP, complex. On the other hand, the remaining bridging energy would still be sufficient to account for the cooperativity in both *deoP2* and *udpP*, for which the ΔG is −2.5 to −3 kcal/mol (*9*, *11*) were it not for a large unfavorable connection free energy change (e.g., +5 kcal/mol).

Finally, how does pairwise cooperativity between CytR binding to CytO and CRP binding to CRP2 of *udpP* survive cytidine binding, particularly when pairwise cooperative interactions with CRP bound to CRP1 of *udpP* or either CRP site of *deoP2* does not? This is not due to direct coupling between cytidine binding to CytR and CytR−CRP association. There may be such coupling, even though it is not evident by the results of sedimentation equilibrium. Such coupling would generate identical effects on ΔG^{o}_{bridge} for *deoP2* and *udpP*, as consistent with our findings. But it would also have same effect on cooperativity, which we know not to be the case. We conclude that the effect of cytidine is mediated through the connection energy for the various complexes (i.e., that cytidine binding affects the additivity of interactions in the three protein complex rather than any of the individual macromolecular interactions).

Perhaps the simplest explanation to tie together these various effects is to suggest that cytidine binding results in conformational changes that reorient the interactions between CytR, CRP, and DNA. A differential effect on cooperativity at different promoters would result depending on how well this matches the scaffold provided by the arrangement of binding motifs for CytR and CRP operators in different promoters. CytR-regulated promoters differ from one another both in spacing between CytR half recognition motifs and in the location of CytO with respect to CRP1 and CRP2. The former varies from 0 to 9 bp and does not match the preferred spacing identified by SELEX experiments. In addition to the obvious differences in distance, the rotational orientations vary over nearly a full helical turn.

For CytR homologues LacR and PurR, the conformational changes that accompany ligand binding are understood from X-ray crystallography (*14*, *44*). In these two cases, binding of inducer and co-repressor, respectively, lead to similar changes in tertiary structure. These alter substantially the dimer interfaces of these proteins to unlock the fixed relative orientation of the two helix−turn−helix, DNA binding domains that interact with the two halves of the palindromic

operators. In this way, ligand binding is linked to DNA binding. In contrast, cytidine binding to CytR is not linked to CytR binding to DNA. It has been argued previously that these processes are uncoupled in CytR because the DNA binding and allosteric Core domains are connected by an unstructured peptide, providing a flexible tether that isolates the DNA-binding domains from structural changes that might occur in the cytidine-binding Core domain (*40*). However, we have demonstrated different modes of site-specific binding to different operators that differ in spacing between recognition half-sites (*45*). This finding is inconsistent with the flexible tether model suggesting instead that CytR assumes distinct conformations that depend on spacing.

Those findings also suggest an interesting correlation between the binding properties and differences in the effect of cytidine binding on cooperativity. The thermodynamics of CytR binding to *deoP2* suggest a relatively more rigid complex whose formation is favored by complementary conformations of CytR and CytO. The thermodynamics of CytR binding to the latter suggest a more flexible complex in which much of the configurational and vibrational freedom of free CytR is retained. The more flexible complex appears less sensitive to effects mediated by cytidine binding since cooperativity is less affected. While intriguing, the small sample size is less than conclusive. The question as to whether the controlling difference between promoters depends on the structure of CytO or on the location of CytO relative to CRP1 and CRP2 is the subject of continuing experiments using synthetic promoter sequences to isolate the two effects. Either outcome highlights the critical role of promoter structure and sequence in directing associations between DNA bound proteins and modulating the regulation of gene expression by those proteins.

ACKNOWLEDGMENT

We would like to acknowledge Steven A. Short both for his invaluable insight and for supplying us with the *udp* promoter containing plasmid. We thank Jim Lee and Angela Gronenborn for the CRP expression strain and Thomas Heyduk for advice on purifying CRP.

REFERENCES

1. Valentin-Hansen, P., Sogaard-Andersen, L., and Pedersen, H. (1996) *Mol. Microbiol. 20*, 461−466.
2. Hammer-Jespersen, K. (1983) in *Metabolism of Nucleotides, Nucleosides and Nucleobases in Microorganisms* (Munch-Petersen, A., Ed.) pp 203−258, Academic Press, London.
3. Weickert, M. J., and Adhya, S. (1992) *J. Biol. Chem. 267*, 15869−15874.
4. Barbier, C. S., Short, S. A., and Senear, D. F. (1997) *J. Biol. Chem. 272*, 16962−16971.
5. Martinussen, J., Mollegaard, N. E., Holst, B., Douthwaite, S. R., and Valentin-Hansen, P. (1989) in *DNA−Protein Interactions in Transcription* (Gralla, J., Ed.) Alan R. Liss, New York.
6. Shin, M., Kang, S., Hyun, S. J., Fujita, N., Ishihama, A., Valentin-Hansen, P., and Choy, H. E. (2001) *EMBO J. 20*, 5392−5399.
7. Busby, S., and Ebright, R. H. (1997) *Mol. Microbiol. 23*, 853−859.
8. Pedersen, H., Sogaard-Andersen, L., Holst, B., Gerlach, P., Bremer, E., and Valentin-Hansen, P. (1992) *J. Mol. Biol. 227*, 396−406.
9. Perini, L. T., Doherty, E. A., Werner, E., and Senear, D. F. (1996) *J. Biol. Chem. 271*, 33242−33255.
10. Pedersen, H., Sogaard-Andersen, L., Holst, B., and Valentin-Hansen, P. (1991) *J. Biol. Chem. 266*, 17804−17808.
11. Gavigan, S. A., Nguyen, T., Nguyen, N., and Senear, D. F. (1999) *J. Biol. Chem. 274*, 16010−16019.
12. Pedersen, H., Dall, J., Dandanell, G., and Valentin-Hansen, P. (1995) *Mol. Microbiol. 17*, 843−853.
13. Sogaard-Andersen, L., and Valentin-Hansen, P. (1993) *Cell 75*, 557−566.
14. Schumacher, M. A., Choi, K. Y., Lu, F., Zalkin, H., and Brennan, R. G. (1995) *Cell 83*, 147−155.
15. Lewis, M., Chang, G., Horton, N. C., Kercher, M. A., Pace, H. C., Schumacher, M. A., Brennan, R. G., and Lu, P. (1996) *Science 271*, 1247−1254.
16. Gronenborn, A. M., and Clore, G. M. (1986) *Biochem. J. 236*, 643−649.
17. Waxman, E., Rusinova, E., Hasselbacher, C. A., Schwartz, G. P., Laws, W. R., and Ross, J. B. (1993) *Anal. Biochem 210*, 425−428.
18. Wetlaufer, D. B. (1962) *Adv. Protein Chem. 17*, 303−390.
19. Senear, D. F., and Batey, R. (1991) *Biochemistry 30*, 6677−6688.
20. Brenowitz, M., Senear, D., Jamison, E., and Dalma-Weiszhausz, D. (1993) in *Footprinting of Nucleic Acid−Protein Complexes* (Revzin, A., Ed.) pp 1−43, Academic Press, Inc., San Diego.
21. Brenowitz, M., and Senear, D. F. (1989) in *Current Protocols in Molecular Biology* (Ausubel, F. M., Brent, R., Kingston, R. E., Moore, D. D., Seidman, J. G., Smith, J. A., and Struhl, K., Eds.) Unit 12.4, Greene Publishing Associates and Wiley-Interscience Associates, New York.
22. Senear, D. F., Perini, L. T., and Gavigan, S. A. (1998) *Methods Enzymol. 295*, 403−424.
23. Senear, D. F., and Bolen, D. W. (1992) *Methods Enzymol. 210*, 463−481.
24. Johnson, M. L., and Faunt, L. M. (1992) *Methods Enzymol. 210*, 1−37.
25. Maniatas, T., Fritsch, E. F., and Sambrook, J. (1989) *Molecular Cloning—A Laboratory Manual*, 2nd ed., Cold Spring Harbor Laboratory, Cold Spring Harbor, NY.
26. Senear, D. F., Ross, J. B., and Laue, T. M. (1998) *Methods 16*, 3−20.
27. Yphantis, D. A. (1964) *Biochemistry 3*, 297−317.
28. Johnson, M. L., Correia, J. J., Yphantis, D. A., and Halvorson, H. R. (1981) *Biophys. J. 36*, 575−588.
29. Yphantis, D. A., and Waugh, D. F. (1956) *J. Phys. Chem. 60*, 623−635.
30. Laue, T. M., Shah, B. D., Ridgeway, T. M., and Pelletier, S. M. (1992) in *Analytical Ultracentrifugation in Biochemistry and Polymer Science* (Harding, S., and Rowe, A., Eds.) pp 90−125, Royal Society of Chemistry, London.
31. Laue, T. M., Anderson, C. F., and Demaine, P. D. (1994) *Prog. Colloid Polym. Sci. 94*, 74−81.
32. Arakawa, T., Hsu, Y. R., and Yphantis, D. A. (1987) *Biochemistry 26*, 5428−5432.
33. Files, J. G., and Weber, K. (1976) *J. Biol. Chem. 251*, 3386−3391.
34. Holst, B., Sogaard-Andersen, L., Pedersen, H., and Valentin-Hansen, P. (1992) *EMBO J. 11*, 3635−3643.
35. Ackers, G. K., Shea, M. A., and Smith, F. R. (1983) *J. Mol. Biol. 170*, 223−242.
36. Coleman, J., Eaton, S., Merkel, G., Skalka, A. M., and Laue, T. (1999) *J. Biol. Chem. 274*, 32842−32846.
37. Passner, J. M., and Steitz, T. A. (1997) *Proc. Natl. Acad. Sci. U.S.A. 94*, 2843−2847.
38. Jencks, W. P. (1981) *Proc. Natl. Acad. Sci. U.S.A. 78*, 4046−4050.
39. Kallipolitis, B. H., Norregaard-Madsen, M., and Valentin-Hansen, P. (1997) *Cell 89*, 1101−1109.
40. Jorgensen, C. I., Kallipolitis, B. H., and Valentin-Hansen, P. (1998) *Mol. Microbiol. 27*, 41−50.
41. Zhang, W., Ni, H., Capp, M. W., Anderson, C. F., Lohman, T. M., and Record, M. T., Jr. (1999) *Biophys. J. 76*, 1008−1017.
42. Pedersen, H., and Valentin-Hansen, P. (1997) *EMBO J. 16*, 2108−2118.
43. Rusinova, E., Ross, J. B., Laue, T. M., Sowers, L. C., and Senear, D. F. (1997) *Biochemistry 36*, 12994−13003.
44. Bell, C. E., and Lewis, M. (2000) *Nat. Struct. Biol. 7*, 209−214.
45. Tretyachenko-Ladokhina, V., Ross, J. B., and Senear, D. F. (2002) *J. Mol. Biol. 316*, 531−546.

BI0271143